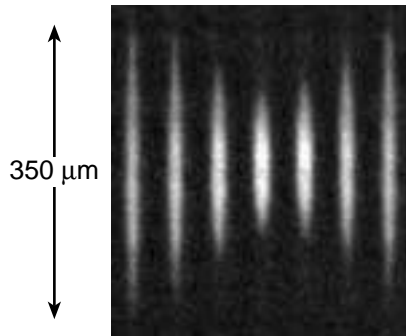


Progress in year 1998

1. Sound at non-zero temperature: collisionless and hydrodynamic excitations of a Bose-Einstein condensate

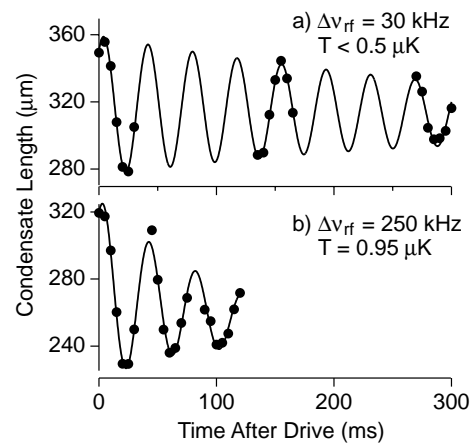
Collective excitations are the fingerprints of a system and reveal many of its dynamic properties. We extended earlier work on collective excitations of a Bose-Einstein condensate by studying them at non-zero temperature and at high density where they become analogous to first and second sound in superfluid helium [1]. The existence of such two modes is characteristic of a superfluid system.

Our study focused on the lowest-lying shape oscillation. This oscillation was probed above and below the Bose-Einstein condensation temperature. The temperature dependencies of the frequency and damping rates of condensate oscillations indicate significant interactions between the condensate and the thermal cloud. First sound, which constitutes hydrodynamic oscillations of the thermal cloud, was observed. An antisymmetric dipolar oscillation of the thermal cloud and the condensate was also studied. This excitation represents the bulk flow of a superfluid through the normal fluid and has similarities to second sound. The detailed theoretical description of these results is currently a challenge for many-body theorists.



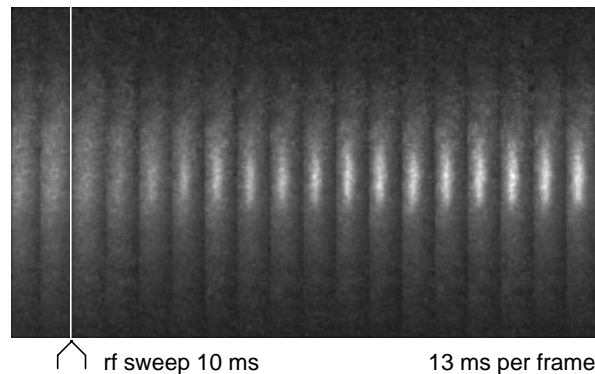
Damped quadrupolar condensate oscillations at low (a) and high (b) temperature. Points show the axial condensate length determined from fits to phase-contrast images (such as shown in the figure above). The oscillation at high temperature has a slightly lower frequency, and is damped more rapidly than at low temperature.

In situ images of the $m=0$ quadrupolar condensate oscillation near 30 Hz. A Bose-Einstein condensate with no discernible thermal component was imaged every 5 ms by phase-contrast imaging. The evident change in the axial length of the condensate was used to characterize the oscillation.



2. Bosonic stimulation in the formation of a Bose-Einstein condensate

Quantum-mechanical symmetry leads to bosonic stimulation, i.e. the probability of non-condensed atoms scattering into the condensate is proportional to the number of condensed atoms already present. This process is analogous to stimulated emission of photons and can be considered as “matter wave amplification.” When we observed the formation of the condensate after suddenly quenching the cloud below the transition temperature we obtained evidence for bosonic amplification [2]. Bosonic stimulation leads to an acceleration of the rate at which atoms enter the condensate - the formation process therefore starts slowly, speeds up and then approaches equilibrium.



The formation of a Bose-Einstein condensate. Shown is a sequence of 18 phase-contrast images taken in situ of the same condensate. The first two frames show a thermal cloud at a temperature above the transition temperature. The following 16 frames were taken after the cloud was quenched below the BEC transition, and show the growth of a condensate at the center of the cloud at 13 ms intervals. Note the decrease in the number of thermal atoms and their smaller width after the rf sweep. The bright gray levels mark the high column density of the condensate. The length of the images is 630 μm .

3. All-optical confinement of a Bose-Einstein condensate

Magnetic confinement of Bose-Einstein condensates is incompatible with many precision measurements and applications in atom optics. Therefore, we realized an optical trap for a Bose-Einstein condensate [3]. It uses a single, focused infrared laser beam of only a few milliwatts of laser power, which is sufficient due to the very low energy of Bose condensates. In this trap, we have observed high atomic densities which were unprecedented both for Bose condensates and for optically trapped atoms. Furthermore, the trap works at arbitrary magnetic fields and for atoms in all hyperfine states. This has led to the observation of Feshbach resonances and spinor condensates. The optical trap may also serve as an “optical tweezers” to move condensates, and for example, place them close to surfaces and in optical and microwave cavities.

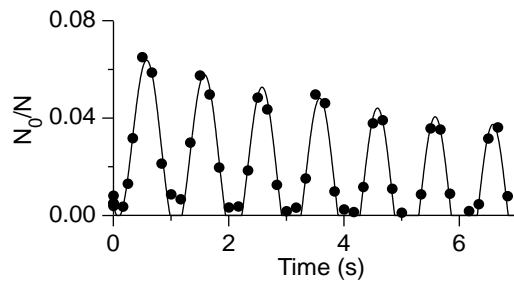
4. Reversible formation of a Bose-Einstein condensate

In an ordinary cryostat, the experimenter can raise and lower the temperature of a sample reversibly. In contrast, evaporative cooling is irreversible due to the loss of the evaporated atoms. Even if the temperature is raised again by (internal or external)

heating of the sample, the number of atoms lost during the cooling stage cannot be recovered.

In recent experiments, we could cross the BEC transition reversibly by slowly changing the shape of the trapping potential using a combination of magnetic and optical forces [4]. This process conserves entropy while changing the local phase space density.

By ramping up the power of an infrared beam focused into the center of the magnetic trap, we could increase the phase-space density by a factor of 50. The reversibility of crossing the BEC phase transition was demonstrated by preparing a magnetically trapped cloud just above the critical temperature and then sinusoidally modulating the infrared power. We could reversibly cycle at least 15 times back and forth across the BEC transition.

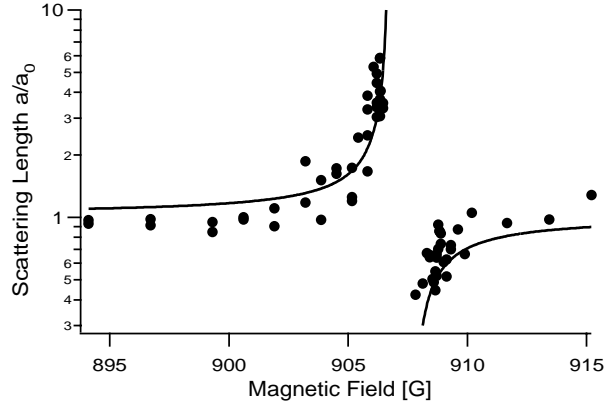


Adiabatic cycling through the phase transition by sinusoidally modulating the optical trapping potential. Shown is the condensate fraction versus time. The solid lines are guides to the eye.

5. Observation of Feshbach resonances in a Bose-Einstein condensate

All the essential properties of Bose condensed systems - the formation and shape of the condensate, the nature of its collective excitations and statistical fluctuations, the formation and dynamics of solitons and vortices - are determined by the strength of the atomic interactions. In atomic gases, the strength of the interaction, characterized by the scattering length, varies dispersively near a Feshbach resonance which occurs at a specific value of the external magnetic field.

Our recent observation of Feshbach resonances in an optically trapped condensate [5] was the first such observation for cold atoms. The strength of the interaction was inferred from the measured release energy. The figure clearly displays the predicted dispersive shape and shows evidence for a variation in the scattering length by more than a factor of ten. Our observation of the dispersive variation of the scattering length confirms the theoretical predictions about “tunability” of the scattering length with the prospect of “designing” atomic quantum gases with novel properties.



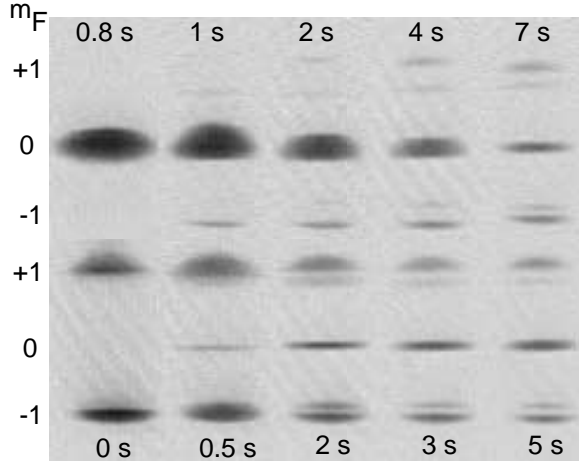
Observation of the Feshbach resonance at a magnetic field of 907 G using time-of-flight absorption imaging. The figure shows the normalized scattering length versus external magnetic field, together with the predicted shape.

6. Spinor Bose-Einstein condensates in optical traps

We have studied the equilibrium state of spinor condensates in an optical trap [6]. In contrast to magnetically trapped condensates, spinor condensates have the orientation of the spin as a degree of freedom, which can be described by a multi-component wavefunction (one for each magnetic sublevel). In an $F=1$ spinor condensate subject to spin relaxation, two $m_F=0$ atoms can collide and produce a $m_F=1$ and a $m_F=-1$ atom and vice versa. The most dramatic effect was seen when we started with a condensate in a pure $m_F=0$ state. Depending on the external magnetic field, the formation of three domains of $m_F = +1, 0, -1$ atoms was observed.

The figure shows a sequence of images with different dwell times in the optical trap. Starting with either the pure $m_F=0$ component (upper series) or with a 50-50 mixture of the $m_F = \pm 1$ components (lower series), the same equilibrium distribution was reached.

Comparison of such equilibrium distributions to a theoretical model revealed that the spin-dependent interaction $c\vec{F}_1 \cdot \vec{F}_2$ between two sodium atoms in the $F=1$ state is anti-ferromagnetic (i.e. $c > 0$). Furthermore, the experimental results showed clear evidence for the miscibility of $m_F = -1$ and $m_F = +1$ components and the immiscibility of $m_F = \pm 1$ and $m_F = 0$. This opens the possibility for detailed studies of miscible and immiscible multi-component condensates.



Absorption images of spinor condensates released from the optical trap, after 25 ms of ballistic expansion. The different m_F states were separated by an axial field gradient (Stern-Gerlach filter). The images taken after various dwell times in the trap show how the atoms evolved into the same equilibrium distribution although they were initially prepared in a pure $m_F = 0$ state (upper row) or in equally populated $m_F = \pm 1$ states (lower row). The height of the images is 2.7 mm.

7. Analytical description of a trapped semi-ideal Bose-Gas

One focus of research on dilute gas Bose-Einstein condensates is the study of thermodynamic quantities such as the transition temperature to Bose-Einstein condensation, and the condensate fraction. In particular, for the dilute gas Bose condensates, the weak interactions between particles and their low density allows for an accurate theoretical description of the effect of interactions in a many-body system starting from a microscopic understanding of two-particle collisions. In collaboration with Martin Naraschewski, a member of our group (DMS-K) explored the effect of interactions on a trapped partially condensed gas using an intuitive and accessible description of the interactions between the condensed and non-condensed atoms [7]. In this "semi-ideal" picture, interactions between condensed atoms are treated by the simple and verified Thomas-Fermi approximation, while the non-condensed fraction is treated as an ideal gas for which the trapping potential and the chemical potential are altered by repulsion from the condensate. This led to analytical expressions for the condensate fraction and for the density of the trapped gas, which can be used directly in the comparison between theory and experimental data.

1. D.M. Stamper-Kurn, H.-J. Miesner, S. Inouye, M.R. Andrews, and W. Ketterle, Phys. Rev. Lett. **81**, 500 (1998).
2. H.-J. Miesner, D.M. Stamper-Kurn, M.R. Andrews, D.S. Durfee, S. Inouye, and W. Ketterle, Science **279**, 1005 (1998).
3. D.M. Stamper-Kurn, M.R. Andrews, A.P. Chikkatur, S. Inouye, H.-J. Miesner, J. Stenger, and W. Ketterle, Phys. Rev. Lett. **80**, 2027 (1998).
4. D.M. Stamper-Kurn, H.-J. Miesner, A.P. Chikkatur, S. Inouye, J. Stenger, and W. Ketterle, Phys. Rev. Lett. **81**, 2194 (1998).
5. S. Inouye, M.R. Andrews, J. Stenger, H.-J. Miesner, D.M. Stamper-Kurn, and W. Ketterle, Nature **392**, 151 (1998).
6. J. Stenger, S. Inouye, D.M. Stamper-Kurn, H.-J. Miesner, A.P. Chikkatur, and W. Ketterle, Nature **396**, 345 (1998).
7. M. Naraschewski and D.M. Stamper-Kurn, Phys. Rev. A **58**, 2423 (1998).